Cs microcell optical reference with frequency stability in the low 10^{-13} range at 1 s

ANTHONY GUSCHING*, JACQUES MILLO , IVAN RYGER , REMY VICARINI , MOUSTAFA ABDEL HAFIZ , NICOLAS PASSILLY , AND RODOLPHE BOUDOT

FEMTO-ST, CNRS, Université de Franche-Comté, ENSMM, 26 chemin de l'Epitaphe 25030 Besançon Cedex, France
** Corresponding author: anthony.gusching@femto-st.fr*

Compiled March 11, 2023

We describe a high-performance optical frequency reference based on dual-frequency sub-Doppler spectroscopy (DFSDS) using a Cs vapor microfabricated cell and an external-cavity diode laser at 895 nm. Measured against a reference optical signal extracted from a cavity-stabilized laser, the microcell-stabilized laser demonstrates an instability of 3×10^{-13} at 1 s, in agreement with a phase noise of $+40$ dBrad^2/Hz at 1 Hz offset frequency, and below 5×10^{-14} at 10^2 s. The laser short-term stability limit is in good agreement with the intermodulation effect from the laser frequency noise. These results suggest that DFSDS is a valuable approach for the development of ultra-stable microcell-based optical standards.

OCIS codes: (300.6320) Spectroscopy, high-resolution; (120.0120) Instrumentation, measurement, and metrology; (020.0020) Atomic and molecular physics; (020.1670) Coherent optical effects; (250.0250) Optoelectronics; (140.0140) Lasers and laser optics;

http://dx.doi.org/10.1364/ao.XX.XXXXXX

Best optical atomic clocks, which rely on the frequency stabilization of a laser onto the ultra-narrow optical transition of laser cooled and lattice-trapped atoms, achieve unprecedented fractional frequency instabilities in the low 10^{-19} range [1–4]. These exceptionally-precise instruments permit to envision a new definition of the SI second [5], enable geodesy below the centimeter level [6, 7] by probing the gravitational red shift [8], test fundamental laws of nature [9, 10], and might contribute to the detection of gravitational waves [11] or dark matter [12]. However, these clocks are bulky and complex, making their deployment outside the laboratory challenging and limited to a restricted number of mobile demonstrators [13].

For applications that require compactness and low-power consumption while being less stringent in terms of fractional frequency stability, thermal cell-based optical frequency references, that benefit from a higher operation frequency than their microwave counterparts [14, 15], constitute an attractive alternative option [16]. Sub-Doppler spectroscopy approaches, that rely on the interaction of thermal atoms or molecules with two counter-propagating laser beams in a cell, have met a remarkable success, including in space applications [17]. With the significant progress in microelectromechanical systems (MEMS) cell technologies and integrated photonics, these methods have known, over the last years, a significantly-renewed interest towards the development of chip-scale optical clocks.

Saturated absorption spectroscopy (SAS) [18], widely-used with glass-blown cells [19, 20], was used to stabilize the frequency of a distributed-Bragg resonator (DBR) laser at the 10^{-11} level up to 10^4 s, with Rb atoms in a microfabricated cell [21]. In [22], a fully-integrated optical frequency reference using SAS in a glass-blown Rb cell with a DBR laser, was demonstrated with a stability of 1.4×10^{-12} at 1 s and better than 10^{-11} at 1 day. Also, stabilization of an external-cavity diode laser (ECDL) on the Cs atom $6S_{1/2}$ - $7P_{1/2}$ transition at 459 nm was demonstrated, achieving the level of 2.1×10^{-13} at 1 s in a 5-cm long cell [23].

Doppler-free two-photon spectroscopy of the $5S_{1/2}$ - $5D_{5/2}$ transition at 778 nm in Rb vapor [24, 25] is also attractive. This method led to the demonstration of a Rb optical clock with a frequency stability of 4×10^{-13} at 1 s and 7×10^{-15} at 1 day [26]. The same transition explored in a MEMS Rb cell [27] yielded an Allan deviation at 1 s of 2.9×10^{-12} with a DBR laser [28] and 1.8×10^{-13} with an ECDL [29]. Prototypes using the 780-776 nm Rb two-photon transition were demonstrated [30].

Dual-frequency sub-Doppler spectroscopy (DFSDS) was also proposed [31, 32]. In this method, atoms in a cell interact with two counter-propagating dual-frequency laser fields, implying, for the specific class of atoms with velocities orthogonal to the laser beams, the destruction of hyperfine and Zeeman dark states, and leading to the detection of high-contrast sign-reversed sub-Doppler resonances. With this approach, a laser

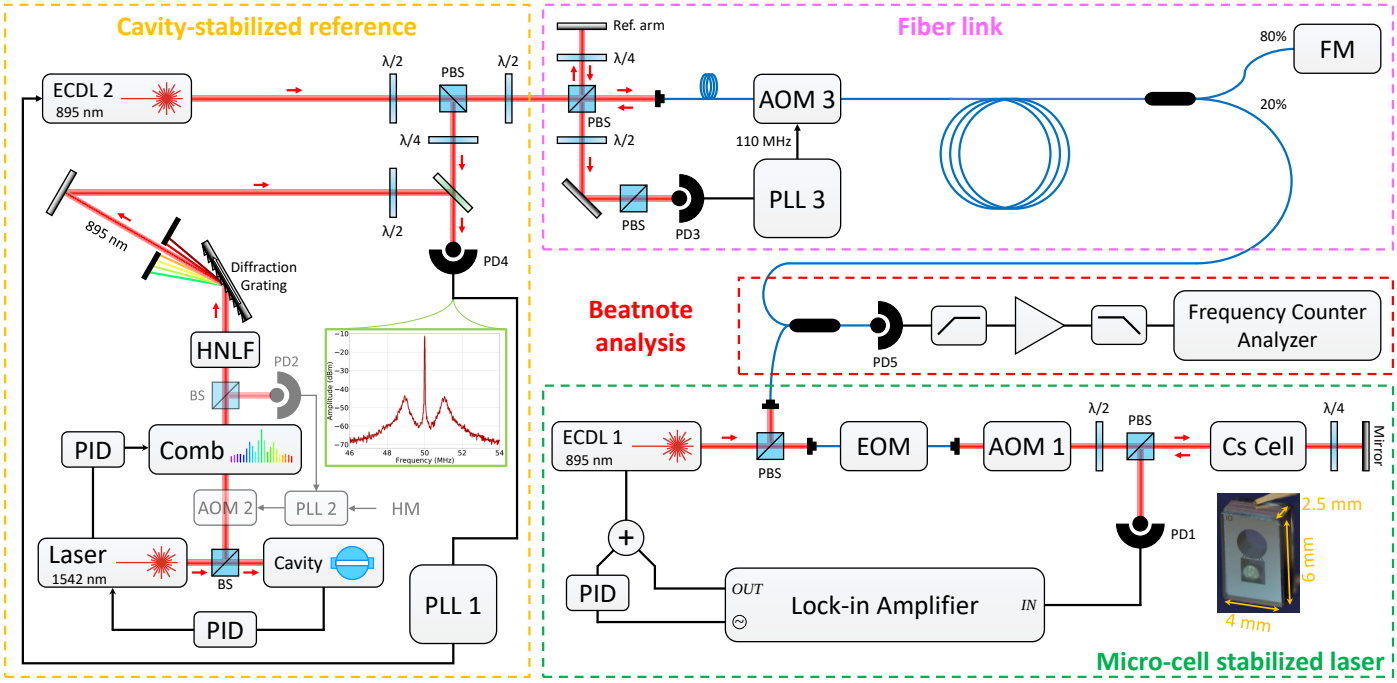

Fig. 1. Experimental set-up for characterization of the microcell-stabilized ECDL 1. The ECDL 2, tuned at 895 nm, is phase-locked to the 895 nm-tooth line of an optical frequency comb phase-locked to a cavity-stabilized laser. The ECDL 2 signal is then transferred to a neighboring lab using a low-noise compensated fiber link, at the output of which a beatnote signal, obtained with the microcell-stabilized ECDL 1, can be counted and analyzed. For stability and frequency shift measurements, the cavity-stabilized laser could be phase-locked to an active hydrogen maser (HM) for improved stability after 100 s. ECDL: external-cavity diode laser, NLF: non-linear fiber, PLL: phase-locked loop, PID: proportional-integral correction, PBS: polarizing beam splitter, PD: photodiode, AOM: acousto-optic modulator, FM: Faraday mirror.

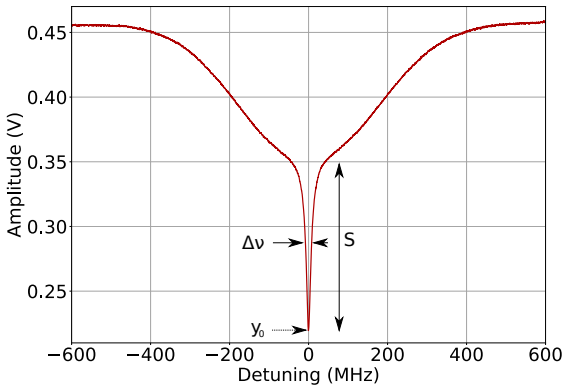

Fig. 2. Sub-Doppler resonance detected in the Cs microfabricated cell using DFSDS. The sub-Doppler resonance exhibits a signal amplitude S of 127 mV, a linewidth $\Delta\nu$ of 15.6 MHz, and a contrast $C = S/y_0 = 0.57$, with y_0 the signal level at the bottom of the sub-Doppler resonance.

beatnote between microcell-stabilized lasers achieved a stability of 1.1×10^{-12} at 1 s [33]. In this study, stability of an ECDL was limited by the laser frequency-modulation (FM) noise through the intermodulation effect [34], due to application of a relatively small modulation frequency ($f_M \sim 62$ kHz).

In this Letter, we report on the characterization of a narrow-linewidth 895 nm ECDL stabilized onto a Cs MEMS cell using DFSDS. A higher modulation frequency (1 MHz) is now used. Measured against an ultra-stable 895 nm signal extracted from an optical frequency comb phase-locked to a cavity-stabilized laser, an Allan deviation of 3×10^{-13} at 1 s, averaging down below 5×10^{-14} at 100 s, is obtained. The stability at 1 s, in agreement with the laser beatnote phase noise of $+40$ dBrad^2/Hz at 1 Hz offset frequency, remains limited by the intermodulation effect [34] from the ECDL FM noise.

Figure 1 shows a schematic of the experimental setup. The microcell-laser is based on the commercial ECDL 1, with 70 dB of optical isolation at the output. The laser field is modulated at 4.596 GHz by driving a fibered Mach-Zehnder electro-optic modulator (EOM) with a microwave frequency synthesizer, such that two first-order optical sidebands frequency-split by 9.192 GHz are obtained. Active carrier suppression is achieved by tuning finely the EOM bias voltage [35]. An acousto-optic modulator (AOM 1), placed at the output of the EOM, is used to control the total laser power. The laser light is sent through a pill dispenser-based Cs vapor microfabricated cell [36]. Atom-light interaction takes place in a 4.7 mm^3 cylindrical silicon-etched cavity. The cell is housed in a cm-scale temperature-controlled duralumin holder and surrounded by a mu-metal shield. At the cell output, the light is reflected back by a mirror to provide orthogonally-polarized counter-propagating laser beams, and directed by a polarizing beam splitter (PBS) to a photodiode (PD1) that delivers the sub-Doppler atomic resonance signal, shown in Fig. 2. An error signal, obtained through synchronous modulation-demodulation technique (frequency $f_M = 1$ MHz), is then extracted and processed in a proportional-integral (PI) controller to correct the laser dc current and piezo actuator for stabilization of the laser frequency onto the atomic resonance.

The characterization of the ECDL 1 is performed by comparing

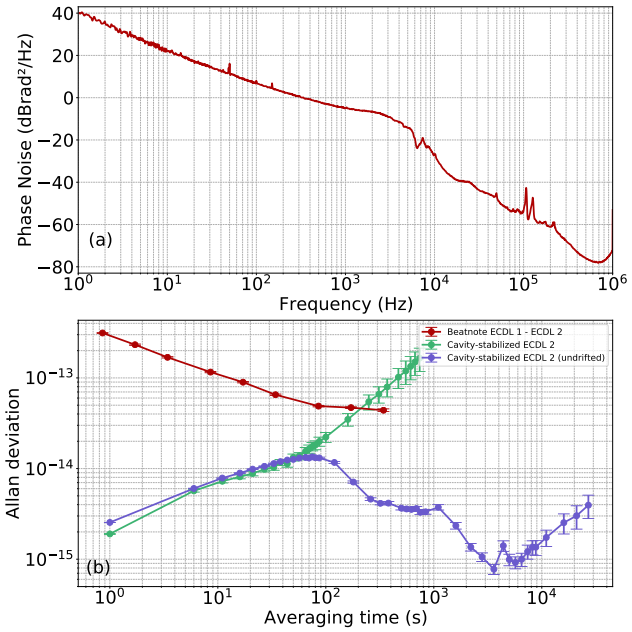

Fig. 3. (a) Phase noise of the laser beatnote between the ECDL 1 and ECDL 2, in locked conditions. (b) Overlapping Allan deviation of the laser beatnote between the ECDL 1 and the ECDL 2 (red curve). The Allan deviation of the cavity-stabilized laser was measured at 10 GHz by frequency-dividing the optical signal with a frequency comb, and making the comparison with a cryogenic sapphire oscillator (CSO). In the first case (green curve), the 1542 nm laser is only stabilized to the ULE reference cavity. In the second case (blue curve), the phase of this laser is also steered by the phase of a hydrogen maser to suppress the drift of the cavity. In this test, the stability degradation after 3000 s is due to the CSO.

its output signal to an ultra-stable 895 nm optical reference signal. A laser tuned at $\lambda = 1542$ nm is first frequency-stabilized to an ultra-stable ultra-low expansion (ULE) glass cavity [37]. A fiber-based femtosecond laser, with a repetition rate of 250 MHz, is fully stabilized using two phase-locked loops (PLL): one to lock the repetition rate signal onto the cavity-stabilized laser and a second one to control the carrier-envelop-offset signal frequency using a hydrogen maser (HM). The optical frequency comb emitted by this laser is amplified and sent into a highly non-linear fiber (HNLF), at the output of which an optical grating is used to extract light power around $\lambda = 895$ nm. This signal is sent to the photodiode PD4. The local ECDL 2, tuned at $\lambda = 895$ nm, is then phase-locked onto the comb mode. A Doppler-compensated fiber-link, shown on Fig. 1, based on a Michelson-type interferometer and comparable to the one described in [38], was then implemented to transfer the cavity-stabilized ECDL 2 signal to the neighboring (~ 20 m) ECDL 1 laboratory room. Ultimately, the beatnote obtained with the fast photodiode PD5 between the ECDL 1 and the ECDL 2 is band-pass filtered, amplified and analyzed with a frequency counter or phase noise analyzer.

Figure 3(a) shows the absolute phase noise of the laser beatnote between the ECDL 1 and ECDL 2, in locked conditions. In the 1 - 10 Hz region, the phase noise spectrum exhibits a f^{-2} slope, signature of white frequency noise, yielding $+40$ dBrad^2/Hz at $f = 1$ Hz, from which an Allan deviation of 3×10^{-13} at 1 s [39] can be predicted. The residual phase noise of the compensated fiber-link was measured to be orders of magnitude lower than the microcell-stabilized ECDL 1, at the level of -57 dBrad^2/Hz at $f = 1$ Hz, comparable with the one obtained in [38].

The Allan deviation of the laser beatnote, shown in Fig. 3(b) (red curve), is in good agreement with the phase noise measurement. It is measured to be 3×10^{-13} at 1 s, averaging down below 5×10^{-14} at 100 s. The laser stability was found to be degraded for integration times higher than a few 100 s. Misalignments between both counter-propagating beams are suspected to be an important contribution to this degradation [40]. The fractional frequency stability of the comb stabilized on the 1542 nm reference laser was evaluated by extracting a low noise 10 GHz signal [41] from the comb and beating it with a cryogenic sapphire oscillator (CSO) (green curve in Fig. 3(b)). From that beatnote, we observe a drift of $\sim 10^{-16}\ \tau$ attributed to the reference ULE cavity that significantly contributes to the evaluation of the microcell-laser after ~ 100 s. To overcome this limitation, a drift compensation system of the reference laser, based on a comparison through the fs laser with the highly stable phase of an hydrogen maser signal, was implemented. The control loop is closed with a time constant of about 100 s and acts on the modulation frequency of the AOM 2. The improvement on the stability of the comb is reported on Fig. 3(b) (in blue). In this case, the comb laser instability is clearly lower than the microcell-laser, ensuring that the performance of the microcell-laser is well identified. In this measurement, the stability degradation for integration times higher than 4×10^3 s is due to the CSO.

We have established the short-term noise budget of the ECDL 1. The latter is reported in Table 1. The main contribution to the stability at 1 s of the ECDL 1 is the intermodulation effect induced by the ECDL FM noise. This contribution, extracted from a measured laser phase noise of -86 dBrad^2/Hz at $f = 2f_M = 2$ MHz, is estimated at 1.5×10^{-13} [33]. Next main noise contributions are estimated one order of magnitude below, in the low 10^{-14} range. This analysis suggests that a significant margin of progress still exists for improving the stability of such microcell-stabilized atomic frequency references. In this domain, the use of ultra-narrow pre-stabilized chip-scale lasers with reduced FM noise [42, 43] appears as an attractive research path to explore.

In conclusion, we have demonstrated the frequency stabilization of an ECDL at 895 nm onto a Cs microfabricated cell using DFSDS. The laser exhibits a phase noise of $+40$ dBrad^2/Hz at 1 Hz offset frequency, and a fractional frequency stability of

Table 1. Contributions of main noise sources to the short-term stability of the microcell-stabilized ECDL 1. Methodology and formula reported in [33] are used
. The laser power at the cell input is 450 μW. PD dark: photodetector noise in the dark. AM noise: amplitude modulation noise.

Noise source	σ (1 s)
Shot noise	3.5×10^{-15}
PD dark	1.5×10^{-14}
Laser AM-AM noise	2.8×10^{-14}
Laser FM-AM noise	3×10^{-14}
Intermodulation	1.5×10^{-13}
σ_y (1 s)	1.5×10^{-13}

3×10^{-13} at 1 s and better than 5×10^{-14} at 100 s. The main contribution to the short-term stability of the microcell-ECDL is the intermodulation effect. The stability at 1 s of the microcell-ECDL approaches the one demonstrated with the two-photon transition at 778 nm in a Rb microcell [29] and demonstrates that the DFSDS technique is a valuable technique for the development of high-stability microcell-based optical references.

FUNDING

This work was supported by Centre National d'Etudes Spatiales (CNES) through the OSCAR project (grant 200837/00), by Région de Franche-Comté (NOUGECELLL project, grant 20174-06245), and by Agence Nationale de la Recherche (ANR) in the frame of the LabeX FIRST-TF (Grant ANR 10-LABX-0048), EquipX Oscillator-IMP (Grant ANR 11-EQPX-0033) and EIPHI Graduate school (Grant ANR-17-EURE-0002) through the REMICS project. The authors thank the French RENATECH network and its FEMTO-ST technological facility.

DISCLOSURES

The authors declare no conflicts of interest.

DATA AVAILABILITY STATEMENT

The data that support the findings of this study are available from the corresponding author upon reasonable request.

REFERENCES

1. A. Ushijima, M. Takamoto, M. Das, T. Okhubo, and H. Katori, Nat. Photon. **9,** 185 (2015).
2. M. Schioppo, R. C. Brown, W. F. McGrew, N. Hinkley, R. J. Fasano, K. Beloy, T. H. Yoon, G. Milani, D. Nicolodi, J. A. Sherman, N. B. Phillips, C. W. Oates and A. Ludlow, Nat. Photon. **11,** 48 (2017).
3. S. M. Brewer, J. S. Chen, A. M. Hankin, E. R. Clements, C. W. Chou, D. J. Wineland, D. B. Hume and D. R. Leibrandt, Phys. Rev. Lett. **123,** 033201 (2019).
4. E. Oelker, R. B. Hutson, C. Kennedy, L. Sonderhouse, T. Bothwell, A. Goban, D. Kedar, C. Sanner, J. M. Robinson, E. Marti, D. G. Matei, T. Legero, M. Giunta, R. Holzwarth, F. Riehle, U. Sterr, and J. Ye, Nat. Photon. **13,** 714 (2019).
5. S. Bize, C. R. Phys. **20,** 153 (2019).
6. W. F. McGrew, X. Zhang, R. J. Fasano, S. A. Schäffer, K. Beloy, D. Nicolodi, R. C. Brown, N. Hinkley, G. Milani, M. Schioppo, T. H. Yoon, and A. D. Ludlow, Nature **564,** 87 (2018).
7. J. Grotti, S. Koller, S. Vogt, S. Häfner, U. Sterr, C. Lisdat, H. Denker, C. Voigt, L. Timmen, A. Rolland, F. N. Baynes, H. S. Margolis, M. Zampaolo, P. Thoumany, M. Pizzocaro, B. Rauf, F. Bregolin, A. Tampellini, P. Barbieri, M. Zucco, G. A. Constanzo, C. Clivati, F. Levi and D. Calonico, Nat. Phys. **14,** 437 (2018).
8. T. Bothwell, C. Kennedy, A. Aeppli, D. Kedar, J. Robinson, E. Oelker, A. Staron, and J. Ye, Nature **602,** 420 (2022).
9. M. Takamoto, I. Ushijima, N. Ohmae, T. Yahagi, K. Kokado, H. Shinkai, and H. Katori, Nat. Photon. **14,** 411 (2020).
10. M. S. Safronova, D. Budker, D. DeMille, D.F.J. Kimball, A. Derevianko, C.W. Clark, Rev. Mod. Phys. **90,** 025008 (2018).
11. S. Kolkowitz I. Pikovski, N. Langellier, M. D. Lukin, R. L. Walsworth, and J. Ye, Phys. Rev. D **94,** 124043 (2016).
12. C. Kennedy, E. Oelker, J. M. Robinson, T. Bothwell, D. Kedar, W. Milner, E. Marti, A. Derevianko, and J. Ye, Phys. Rev. Lett. **125,** 201302 (2020).
13. M. Takamoto, Y. Tanaka and H. Katori, Appl. Phys. Lett. **120,** 140502 (2022).
14. S. Micalizio, C. E. Calosso, A. Godone and F. Levi, Metrologia **49,** 4, 425 (2012).
15. M. Abdel Hafiz, G. Coget, M. Petersen, C. E. Calosso, S. Guérandel, E. de Clercq and R. Boudot, Appl. Phys. Lett. **112,** 244102 (2018).
16. B. Jaduszliwer and J. Camparo, GPS Solutions **25,** 1 (2021).
17. T. Schuldt, M. Gohlke, M. Oswald, J. Wust, T. Blomberg, K. Doringshoff, A. Bawamia, A. Wicht, M. Lezius, K. Voss, M. Krutzik, S. Herrmann, E. Kovalchuk, A. Peters and C. Braxmaier, GPS solutions, **25,** 83 (2021).
18. T. W. Hänsch, I. S. Shahin and A. L. Schawlow, Phys. Rev. Lett. **27,** 707 (1971).
19. G. D. Rovera, G. Santarelli and A. Clairon, Rev. Sci. Instr. **65,** 5, 1502 (1994).
20. C. Affolderbach and G. Mileti, Rev. Sci. Instr. **76,** 073108 (2005).
21. M. T. Hummon, S. Kang, D. G. Bopp, Q. Li, D. A. Westly, S. Kim, C. Fredrick, S. A. Diddams, K. Srinivasan, V. Aksyuk and J. E. Kitching, Optica **5,** 443 (2018).
22. A. Strangfeld, B. Wiegand, J. Kluge, M. Schoch and M. Krutzik, Opt. Express **30,** 12039 (2022).
23. J. Miao, T. Shi, J. Zhang and J. Chen, Phys. Rev. Appl. **18,** 024034 (2022).
24. L. S. Vasilenko, V. P. Chebotaev and A. V. Shishaev, JETP Lett. **12,** 161 (1970).
25. F. Nez, F. Biraben, R. Felder and Y. Millerioux, Opt. Commun. **102,** 432 (1993).
26. N. D. Lemke, K. W. Martin, R. Beard, B. K. Stuhl, A. J. Metcalf and J. D. Elgin, MDPI Sensors **22,** 1982 (2022).
27. Z. L. Newman, V. Maurice, T. Drake, J. R. Stone, T. C. Briles, D. T. Spencer, C. Fredrick, Q. Li, D. Westly, B. R. Ilic, B. Shen, M.-G. Suh, K. Y. Yang, C. Johnson, D. M. S. Johnson, L. Hollberg, K. J. Vahala, K. Srinivasan, S. A. Diddams, J. Kitching, S. B. Papp, and M. T. Hummon, Optica **6,** 680 (2019).
28. V. Maurice, Z. L. Newman, S. Dickerson, M. Rivers, J. Hsiao, P. Greene, M. Mescher, J. Kitching, M. T. Hummon and C. Johnson, Opt. Express **28,** 24708 (2020).
29. Z. L. Newman, V. Maurice, C. Fredrick, T. Fortier, H. Leopardi, L. Hollberg, S. A. Diddams, J. Kitching, and M. T. Hummon, Opt. Lett. **46,** 4702 (2021).
30. C. Perrella, P.S. Light, J.D. Anstie, F.N. Baynes, R.T. White, and A.N. Luiten, Phys. Rev. Appl. **12,** 054063 (2019).
31. M. Abdel Hafiz, G. Coget, E. de Clercq and R. Boudot, Opt. Lett. **41,** 2982 (2016).
32. D. V. Brazhnikov, M. Petersen, G. Coget, N. Passilly, V. Maurice, C. Gorecki and R. Boudot, Phys. Rev. A **99,** 062508 (2019).
33. A. Gusching, M. Petersen, N. Passilly, D. Brazhnikov, M. Abdel Hafiz, and R. Boudot, J. Opt. Soc. Am. B **38,** 3254 (2021).
34. C. Audoin, V. Candelier and N. Dimarcq, IEEE Trans. Instr. Meas. **40,** 2, 121 (1991).
35. X. Liu, J. M. Merolla, S. Guérandel, C. Gorecki, E. de Clercq and R. Boudot, Phys. Rev. A **97,** 013416 (2013).
36. R. Vicarini, V. Maurice, M. Abdel Hafiz, J. Rutkowski, C. Gorecki, N. Passilly, L. Ribetto, V. Gaff, V. Volant, S. Galliou and R. Boudot, Sens. Actuat.: Phys. A **280,** 99 (2018).
37. A. Didier, J. Millo, S. Grop, B. Dubois, E. Bilger, E. Rubiola, C. Lacroute and Y. Kersalé, Appl. Opt. **54,** 12, 3682 (2015).
38. S. Mukherjee, J. Millo, B. Marechal, S. Denis, G. Goavec-Merou, J. M. Friedt, Y. Kersalé, C. Lacroute, IEEE Trans. Ultrason. Ferroelec. Freq. Contr. **69,** 2, 878 (2022).
39. E. Rubiola and F. Vernotte, ArXiv 2201.07109 (2022).
40. C. Affolderbach and G. Mileti, Opt. Lasers Eng. **41,** 291 (2005).
41. C. Fluhr, S. Grop, B. Dubois, Y. Kersalé, E. Rubiola and V. Giordano, IEEE Trans. Ultrason. Ferroelec. Freq. Contr. **63,** 6, 915 (2016).
42. C. A. McLemore, N. Jin, M. L. Kelleher, J. P. Hendrie, D. Mason, Y. Luo, D. Lee, P. Rakich, S. A. Diddams, and F. Quinlan, Phys. Rev. Appl. **18,** 054054 (2022).
43. M. Corato-Zanarella, A. Gil-Molina, X. Ji, M. C. Shin, A. Mohanty and M. Lipson, Nature Photonics **17,** 157 (2023).

REFERENCES

1. A. Ushijima, M. Takamoto, M. Das, T. Okhubo, and H. Katori, Cryogenic optical lattice clocks, Nat. Photon. **9,** 185 (2015).
2. M. Schioppo, R. C. Brown, W. F. McGrew, N. Hinkley, R. J. Fasano, K. Beloy, T. H. Yoon, G. Milani, D. Nicolodi, J. A. Sherman, N. B. Phillips, C. W. Oates and A. Ludlow, Ultra-stable optical clock with two cold-atom ensembles, Nat. Photon. **11,** 48 (2017).
3. S. M. Brewer, J. S. Chen, A. M. Hankin, E. R. Clements, C. W. Chou, D. J. Wineland, D. B. Hume and D. R. Leibrandt, $^{27}Al^{+}$ quantum-logic clock with a systematic uncertainty below 10^{-18}, Phys. Rev. Lett. **123,** 033201 (2019).
4. E. Oelker, R. B. Hutson, C. Kennedy, L. Sonderhouse, T. Bothwell, A. Goban, D. Kedar, C. Sanner, J. M. Robinson, E. Marti, D. G. Matei, T. Legero, M. Giunta, R. Holzwarth, F. Riehle, U. Sterr, and J. Ye, Demonstration of 4.8×10^{-17} stability at 1 s for two independent optical clocks, Nat. Photon. **13,** 714 (2019).
5. S. Bize, The unit of time: Present and future directions, C. R. Phys. **20,** 153 (2019).
6. W. F. McGrew, X. Zhang, R. J. Fasano, S. A. Schäffer, K. Beloy, D. Nicolodi, R. C. Brown, N. Hinkley, G. Milani, M. Schioppo, T. H. Yoon, and A. D. Ludlow, Atomic clock performance enabling geodesy below the centimeter level, Nature **564,** 87 (2018).
7. J. Grotti, S. Koller, S. Vogt, S. Häfner, U. Sterr, C. Lisdat, H. Denker, C. Voigt, L. Timmen, A. Rolland, F. N. Baynes, H. S. Margolis, M. Zampaolo, P. Thoumany, M. Pizzocaro, B. Rauf, F. Bregolin, A. Tampellini, P. Barbieri, M. Zucco, G. A. Constanzo, C. Clivati, F. Levi and D. Calonico, Geodesy and metrology with a transportable optical clock, Nat. Phys. **14,** 437 (2018).
8. T. Bothwell, Kennedy, C., Aeppli, A., Kedar, D., Robinson, J., Oelker, E., Staron, A., and Ye, Resolving the gravitational redshift across a millimetre-scale atomic sample, Nature **602,** 420 (2022).
9. M. Takamoto, I. Ushijima, N. Ohmae, T. Yahagi, K. Kokado, H. Shinkai, and H. Katori, Test of general relativity by a pair of transportable optical lattice clocks, Nat. Photon. **14,** 411 (2020).
10. M. S. Safronova, D. Budker, D. DeMille, D.F.J. Kimball, A. Derevianko, C.W. Clark, Search for new physics with atoms and molecules, Rev. Mod. Phys. **90,** 025008 (2018).
11. S. Kolkowitz I. Pikovski, N. Langellier, M. D. Lukin, R. L. Walsworth, and J. Ye, Gravitational wave detection with optical lattice atomic clocks, Phys. Rev. D **94,** 124043 (2016).
12. C. Kennedy, E. Oelker, J. M. Robinson, T. Bothwell, D. Kedar, W. Milner, E. Marti, A. Derevianko, and J. Ye, Precision metrology meets cosmology: Improved constraints on ultralight dark matter from atom-cavity frequency comparisons, Phys. Rev. Lett. **125,** 201302 (2020).
13. M. Takamoto, Y. Tanaka and H. Katori, A perspective on the future of transportable optical lattice clocks, Appl. Phys. Lett. **120,** 140502 (2022).
14. S. Micalizio, C. E. Calosso, A. Godone and F. Levi, Metrological characterization of the pulsed Rb clock with optical detection, Metrologia **49,** 425 (2012).
15. M. Abdel Hafiz, G. Coget, M. Petersen, C. E. Calosso, S. Guérandel, E. de Clercq and R. Boudot, Symmetric autobalanced Ramsey interrogation for high-performance coherent population-trapping vapor-cell atomic clock, Appl. Phys. Lett. **112,** 244102 (2018).
16. B. Jaduszliwer and J. Camparo, Past, present and future of atomic clocks for GNSS, GPS Solutions **25,** 1 (2021).
17. T. Schuldt, M. Gohlke, M. Oswald, J. Wust, T. Blomberg, K. Doringshoff, A. Bawamia, A. Wicht, M. Lezius, K. Voss, M. Krutzik, S. Herrmann, E. Kovalchuk, A. Peters and C. Braxmaier, Optical clock technologies for global navigation satellite systems, GPS solutions, **25,** 83 (2021).
18. T. W. Hänsch, I. S. Shahin and A. L. Schawlow, High-resolution saturation spectroscopy of the sodium D lines with a pulsed tunable dye laser, Phys. Rev. Lett. **27,** 707 (1971).
19. G. D. Rovera, G. Santarelli and A. Clairon, A laser diode system stabilized on the cesium D2 line, Rev. Sci. Instr. **65,** 1502 (1994).
20. C. Affolderbach and G. Mileti, A compact laser head with high-frequency stability for Rb atomic clocks and optical instrumentation Rev. Sci. Instr. **76,** 073108 (2005).
21. M. T. Hummon, S. Kang, D. G. Bopp, Q. Li, D. A. Westly, S. Kim, C. Fredrick, S. A. Diddams, K. Srinivasan, V. Aksyuk and J. E. Kitching, Photonic chip for laser stabilization to an atomic vapor with 10^{-11} instability, Optica **5,** 443 (2018).
22. A. Strangfeld, B. Wiegand, J. Kluge, M. Schoch and M. Krutzik, Compact plug and play optical frequency reference device based on Doppler-free spectroscopy of rubidium vapor, Opt. Express **30,** 12039 (2022).
23. J. Miao, T. Shi, J. Zhang and J. Chen, Compact 459 nm Cs cell optical frequency standard with $2.1 \times 10^{-13}/\sqrt{\tau}$ short-term stability, Phys. Rev. Appl. **18,** 024034 (2022).
24. L. S. Vasilenko, V. P. Chebotaev and A. V. Shishaev, Line shape of two-photon absorption in a standing-wave field in a gas, JETP Lett. **12,** 161 (1970).
25. F. Nez, F. Biraben, R. Felder and Y. Millerioux, Optical frequency determination of the hyperfine components of the 5S1/2 – 5D3/2 two-photon transitions in rubidium, Opt. Comm. **102,** 432 (1993).
26. N. D. Lemke, K. W. Martin, R. Beard, B. K. Stuhl, A. J. Metcalf and J. D. Elgin, Measurement of Optical Rubidium Clock Frequency Spanning 65 Days, MDPI Sensors **22,** 1982 (2022).
27. Z. L. Newman, V. Maurice, T. Drake, J. R. Stone, T. C. Briles, D. T. Spencer, C. Fredrick, Q. Li, D. Westly, B. R. Ilic, B. Shen, M.-G. Suh, K. Y. Yang, C. Johnson, D. M. S. Johnson, L. Hollberg, K. J. Vahala, K. Srinivasan, S. A. Diddams, J. Kitching, S. B. Papp, and M. T. Hummon, Architecture for the photonic integration of an optical atomic clock, Optica **6,** 680 (2019).
28. V. Maurice, Z. L. Newman, S. Dickerson, M. Rivers, J. Hsiao, P. Greene, M. Mescher, J. Kitching, M. T. Hummon and C. Johnson, Miniaturized optical frequency reference for next-generation portable optical clocks, Opt. Express **28,** 24708 (2020).
29. Z. L. Newman, V. Maurice, C. Fredrick, T. Fortier, H. Leopardi, L. Hollberg, S. A. Diddams, J. Kitching, and M. T. Hummon, High-performance, compact optical standard, Opt. Lett. **46,** 18, 4702 (2021).
30. C. Perrella, P.S. Light, J.D. Anstie, F.N. Baynes, R.T. White, and A.N. Luiten, Dichroic two-photon rubidium frequency standard, Phys. Rev. Appl. **12,** 054063 (2019).
31. M. Abdel Hafiz, G. Coget, E. de Clercq and R. Boudot, Doppler-free spectroscopy on the Cs D1 line with a dual-frequency laser, Opt. Lett. **41,** 2982 (2016).
32. D. V. Brazhnikov, M. Petersen, G. Coget, N. Passilly, V. Maurice, C. Gorecki and R. Boudot, Dual-frequency sub-Doppler spectroscopy: Extended theoretical model and microcell-based experiments, Phys. Rev. A **99,** 062508 (2019).
33. A. Gusching, M. Petersen, N. Passilly, D. Brazhnikov, M. Abdel Hafiz, and R. Boudot, Short-term stability of Cs microcell-stabilized lasers using dual-frequency sub-Doppler spectroscopy, J. Opt. Soc. Am. B **38,** 10, 3254 (2021).
34. C. Audoin, V. Candelier and N. Dimarcq, A limit to the frequency stability of passive frequency standards due to an intermodulation effect, IEEE Trans. Instr. Meas. **40,** 2, 121 (1991).
35. X. Liu, J. M. Merolla, S. Guérandel, C. Gorecki, E. de Clercq and R. Boudot, Coherent-population-trapping resonances in buffer-gas-filled Cs vapor cells with push-pull optical pumping, Phys. Rev. A **97,** 013416 (2013).
36. R. Vicarini, V. Maurice, M. Abdel Hafiz, J. Rutkowski, C. Gorecki, N. Passilly, L. Ribetto, V. Gaff, V. Volant, S. Galliou and R. Boudot, Demonstration of the mass-producible feature of a Cs vapor microcell technology for miniature atomic clocks, Sensors Actuators: Phys. A **280,** 99 (2018).
37. A. Didier, J. Millo, S. Grop, B. Dubois, E. Bilger, E. Rubiola, C. Lacroute and Y. Kersalé, Ultra-low phase noise all-optical microwave generation setup based on commercial devices, Appl. Opt. **54,** 12, 3682 (2015).
38. S. Mukherjee, J. Millo, B. Marechal, S. Denis, G. Goavec-Merou, J. M. Friedt, Y. Kersalé, C. Lacroute, Digital Doppler-cancellation

servo for ultra-stable optical frequency dissemination over fiber, IEEE Trans. Ultrason. Ferroelec. Freq Contr. **69,** 2, 878 (2022).
39. E. Rubiola and F. Vernotte, The companion of the Enrico's chart for phase noise and two-sample Variances, ArXiv 2201.07109 (2022).
40. C. Affolderbach and G. Mileti, Tunable, stabilised diode lasers for compact atomic frequency standards and precision wavelength references, Opt. Lasers Eng. **41,** 291 (2005).
41. C. Fluhr, S. Grop, B. Dubois, Y. Kersalé, E. Rubiola and V. Giordano, Characterization of the individual short-term frequency stability of cryogenic sapphire oscillators at the 10^{-16} level, IEEE Trans. Ultrason. Ferroelec. Freq. Contr. **63,** 6, 915 (2016).
42. C. A. McLemore, N. Jin, M. L. Kelleher, J. P. Hendrie, D. Mason, Y. Luo, D. Lee, P. Rakich, S. A. Diddams, and F. Quinlan, Miniaturizing Ultrastable Electromagnetic Oscillators: Sub-10^{-14} Frequency Instability from a Centimeter-Scale Fabry-Perot Cavity, Phys. Rev. Appl. **18,** 054054 (2022).
43. M. Corato-Zanarella, A. Gil-Molina, X. Ji, M. C. Shin, A. Mohanty and M. Lipson, Widely tunable and narrow-linewidth chip-scale lasers from near-ultraviolet to near-infrared wavelengths, Nature Photonics **17,** 157 (2023).